Heliyon 10 (2024) e31313

Contents lists available at ScienceDirect

Heliyon

journal homepage: www.cell.com/heliyon

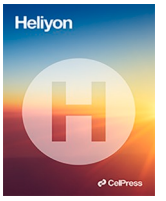

Research article

A single-step extraction and immobilization of soybean lipolytic enzymes by using a purpose-designed copolymer of styrene and maleic acid as a membrane lysis agent

Chatmani Buachi [a], Kamonchanok Thananukul [a], Kitiphong Khongphinitbunjong [a], Robert Molloy [b,c], Patchara Punyamoonwongsa [a,*]

[a] School of Science, Mae Fah Luang University, Chiang Rai, 57100, Thailand
[b] Polymer Research Group, Department of Chemistry, Faculty of Science, Chiang Mai University, Chiang Mai, 50200, Thailand
[c] Materials Science Research Center, Faculty of Science, Chiang Mai University, Chiang Mai, 50200, Thailand

ARTICLE INFO

Keywords:
Styrene maleic acid
Membrane lysis agent
Lipolytic enzymes
Soybean seed
Photopolymerization

ABSTRACT

Approaches aiming to recover proteins without denaturation represent attractive strategies. To accomplish this, a membrane lysis agent based on poly(styrene-*alt*-maleic acid) or PSMA was synthesized by photopolymerization using Irgacure® 2959 and carbon tetrabromide (CBr_4) as a radical initiator and a reversible chain transfer agent, respectively. Structural elucidation of our in-house synthesized PSMA, so-called photo-PSMA, was performed by using NMR spectroscopy. The use of this photo-PSMA in soybean enzyme extraction was also demonstrated for the first time in this study. Without a severe cell rupture, energy input or any organic solvent, recovery of lipolytic enzymes directly into nanometric-sized particles was accomplished in one-step process. Due to the improved structural regularity along the photo-PSMA backbone, the most effective protective reservoir for enzyme immobilization was generated through the PSMA aggregation. Formation of such reservoir enabled soybean enzymes to be shielded from the surroundings and resolved in their full functioning state. This was convinced by the increased specific lipolytic activity to 1,950 mU/mg, significantly higher than those of sodium dodecyl sulfate (SDS) and the two commercially-available PSMA sources (1000P and 2000P). Our photo-PSMA had thus demonstrated its great potential for cell lyse application, especially for soybean hydrolase extraction.

1. Introduction

Plant bioactive compounds are naturally-based substances that display pharmacological effects on humans. They are created as a mean to support biological function of plant metabolites. Among these, lipolytic enzymes, such as lipases and esterases, have received much attention for industrial applications. They are known to catalyze both hydrolysis and the synthesis of ester compounds [1]. Natural lipases hydrolyze triglycerides to obtain monoglycerides, diglycerides, fatty acids and glycerol [2]. Most of lipase molecules have an active core, which separates them from the reaction media. At the oil-water interface, their active lid is fully opened, allowing hydrolysis of oil droplets to be occurred. Esterases however target the ester bonds of water-soluble fatty acid esters with short chain

* Corresponding author.
E-mail address: patchara@mfu.ac.th (P. Punyamoonwongsa).

https://doi.org/10.1016/j.heliyon.2024.e31313
Received 13 January 2024; Received in revised form 13 May 2024; Accepted 14 May 2024
Available online 15 May 2024
2405-8440/© 2024 The Authors. Published by Elsevier Ltd. This is an open access article under the CC BY-NC license (http://creativecommons.org/licenses/by-nc/4.0/).

acyl groups. Ester bond hydrolysis is occurred through the nucleophilic addition of the serine moieties on the carbonyl group of the substrate [3]. Applications of lipolytic enzymes include transesterification of biodiesel production, as well as esterification for cosmetics, food, perfumery and medicine [1,4]. Soybean seeds can be an alternative source of lipolytic enzymes due to their low-cost production, biologically safe and ease of purification. Comparing to microbial sources, they are less toxic even in the partial purified formats. During seed germination, lipases are produced as a mean to break down the stored fats into fatty acids, which later serve as an energy source for embryonic growth and seed development. These enzymes are located within the seed lipid bodies, or attached closely to the biological membranes [5,6].

To extract plant bioactive compounds, the process of membrane solubilization or cell lysis needs to be occurred. Cell membrane is made of thin layer of amphipathic phospholipids together with some other biomolecules, such as proteins, lipids, and carbohydrates. It serves as a protective barrier and regulates the movement of substances across biological cells. For plant protein extraction, the complete cell lysis by using a membrane lysis agent (e.g., detergents, soaps, polymeric surfactants) is preferred due to the cost-effectiveness, ease of operation and high lyse efficiency under mild conditions (pH 6–8). However, the wrong choices of lysis agents can lead to protein denaturation due to a permanent binding with the excess membrane lysis molecules [7,8]. Amphipathic polymers have recently demonstrated their use in transmembrane protein extraction. Among these, poly(styrene-*alt*-maleic acid) or PSMA showed an outstanding character. This copolymer is normally obtained by alkaline hydrolysis of poly(styrene-*alt*-maleic anhydride) (PSMAnh). This precursor is normally synthesized by radical polymerization of styrene (S) and maleic anhydride (MAnh). Due to its amphipathic nature, PSMA can bind with membrane lipid and then induce a micro-pore defect formation within biological membrane, resulting in membrane leakage or even, membrane solubilization to leak out cytoplasmic ingredients [9–12].

Despite this, unmodified PSMA lysis agent has several drawbacks. Its sensitivity to divalent cations (e.g., Ca^{2+}, Mg^{2+}, etc.) [16] can alter stability of a PSMA/lipid vesicle, thus limiting its use in proteomic analysis. Another issue is linked to its optimal polymer chain length to establish the most effective membrane insertion and cell lyse efficiency. According to Morrison and coworkers [12], the low molecular weight PSMA types (<10 kDa) were suggested. To achieve this, suitable chain transfer agents were introduced into the polymerization mixture [13–15]. Tetrabromomethane (CBr_4) is a known chain transfer agent used in radical polymerization because of its relatively high chain transfer constant [16]. At 2 mol% CBr_4, we reported a successful synthesis of low molecular weight PSMAnh via photopolymerization using 2-hydroxy-4′-(2-hydroxyethoxy)-2-methylpropiophenone (Irgacure® 2959) as a photoinitiator. By using a dilute-solution viscometry, the average-molecular weight (M_w) of this photo-PSMAnh was as low as 4.9 x 10^3 g/mol [17], representing an ideal candidate for membrane lysis applications. Whilst ^{1}H-NMR data analysis revealed its copolymer composition of 50:50 (S:MAnh mol%), tendency to form a true alternating S-MAnh patterning has never been explored. The work herein provided an in-depth structural characterization of our photo-PSMA via monitoring triad S-MAnh-S sequencing using the ^{13}C-nuclear magnetic resonance (^{13}C-NMR) spectroscopy. Practical implementation of this copolymer in cell lyse applications was also demonstrated in this study. For this, soybean lipolytic enzymes were selected as a targeted protein due to their great industrial potential. The extraction protocol was a single-step process in an aqueous-based media without the use of toxic organic solvent, energy input or severe cell rupture, thus representing an ideal greener strategy for future large-scale production. Extraction efficiencies were based on the recovery yields, the total sugar and protein contents, as well as the specific lipolytic activity against the *p*-nitrophenyl butyrate (pNPB) substrate. The results were compared with the commercially-available membrane lysis agents, including sodium dodecyl sulfate (SDS), 1000P (molar S/MAnh ratio of 1:1) and 2000P (2:1).

2. Experimental

2.1. Synthesis of PSMAnh precursor

The method was obtained from our previous work [17]. Briefly, styrene (S; 0.075 mol), maleic anhydride (MAnh; 0.075 mol), carbon tetrabromide (CBr_4; 0.0030 mol) and 2-hydroxy-4'-(2-hydroxyethoxy)-2-methylpropiophenone (Irgacure® 2959, 0.0015 mol) were mixed in 150 ml tetrahydrofuran (THF) as a solvent. Therefore, the initial feed composition employed was; [S]:[MAnh] = 1:1 (mol ratio), [S + MAnh] = 1 M, [Irgacure] = 1 mol% and [CBr_4] = 2 mol%. This synthesis condition was previously predetermined and selected based on high yield (~90 %) and suitability in obtaining low molecular weight PSMA product (<10,000 $gmol^{-1}$). Photopolymerization was carried out in a closed conical flask under a nitrogen atmosphere and at room temperature for 6 h. To ensure homogeneity throughout the entire polymerization process, a reaction mixture was constantly stirred with a magnetic bar at 300 rpm. The UV light source was comprised of a series of four 15 Watts UV light tubes (300–415 nm). The copolymer product (photo-PSMAnh) was isolated by precipitation in cold methanol (5-fold excess), and dried to constant weight in a vacuum oven (60 °C).

2.2. Preparation of PSMA lysis agents

The method was adapted from the previous work [17]. Briefly, a 4 g of PSMAnh sample was refluxed gently in 80 ml 0.5 M aqueous sodium hydroxide (NaOH) solution with magnetic stirring for 3 h. The resultant solution (pH 11–12) was left to cool down before neutralization to pH 7–8 by using 0.5 M hydrochloric acid (HCl). The copolymer (PSMA) was isolated by precipitating in chilled acetone (5-fold excess). It was then filtered, washed with a minimum of cold water, and finally dried to a constant weight in a vacuum oven at 60 °C. The product was obtained as an off-white powder with excellent water solubility. A 1 % (w/v) of PSMA aqueous solution showed a pH between 6.5 and 7.5.

2.3. Polymer characterization

Gel permeation chromatograph (GPC) was used to approximate the polymer molecular weight of the PSMAnh precursor. The measurements were performed at 40 °C on Styragel HR5E 7.8 × 300 mm column (Mw 2,000–4,000,000) equipped with Waters 2414 refractive index (RI) detector. The columns were eluted by using THF with a flow rate of 1.0 ml/min and calibrated with poly(styrene) standards. These standards are normally used for the THF-based GPC. It is widely acknowledged that GPC is a relative analytical tool and rather than providing absolute molecular weights, it gives a guide to the size of our polymer chains in THF solution in relative to linear poly(styrene). In our case, given that one of the components in PSMA is poly(styrene), these do seem to be the most appropriate standards to use.

All NMR experiments were carried out on a Bruker AVANCE 500 mHz spectrometer. The hydrolysed sample (10 mg) was dissolved in 1 ml of D_2O for analysis. In DOSY experiment, diffusion coefficient (D) was obtained at room temperature by using a diffusion time of 400 ms and a delay of 50 ms. The measurements were recorded using a 128 scan and an acquisition time of 0.84 s.

2.4. Soybean extraction

A lysis buffer solution containing 1% (w/v) of our photo-PSMA was prepared in 50 mM potassium phosphate buffer (K_2HPO_4/KH_2PO_4). The pH adjustment was made to pH of 7.5 by a slightly addition of 0.5 M HCl or 0.5 M NaOH solution. One gram of soybean seeds (*Glycine max*.) obtained from a local market in Chiangrai was suspended overnight in 25 ml of lysis solution. The soaking liquid (referred to extracted solution) was filtered through a Whatman filter paper (No.1) before freeze-drying. The yield percentage was calculated based on the initial weight of the soybean seeds. To compare the results with the commercially-available sources, the photo-PSMA lysis agent was replaced by sodium dodecyl sulfate (SDS), 1000P (Sartomer®; 1:1) or 2000P (Sartomer®; 2:1). The final concentration for all lysis agents used was fixed at 1% (w/v). The chemical structures of SDS, 2000P and our photo-PSMA (or 1000P) are presented in Fig. 1a, b and c, respectively.

2.5. Analysis of soybean crude extracts

The phenol-sulfuric assay was used to determine the total sugar content in the extracted solutions. The standard glucose solution was initially prepared at 200 μg/ml in Mili-Q water. This standard was diluted to obtain a series solution of 5–200 μg/ml using Mili-Q water as a diluent. Then, 200 μl of the standard solution (or 1.4 mg/ml of the extracted solution) was transferred into a 10 ml test tube, followed by the additions of 200 μl phenol (5%) and 1 ml sulfuric acid (95%), respectively. After 30 min, a 250 μl of the reaction mixture was transferred into a 96-well plate. The solution was measured at 490 nm by using a spectrophotometer (Thermo Fisher Scientific, 4001/4 Genesys20). The results, expressed in the unit of micrograms of sugars per a milliliter of a solution (μg/ml), were obtained based on the glucose calibration plot.

A bicinchoninic acid assay (BCA) was used to determine the total protein content in the extracted solutions. A series solution of bovine serum albumin (BSA) at the concentrations between 4 and 125 μg/ml was prepared in Milli-Q water. Into the 96-well plate, a 10 μl of the BSA solution (or 1.4 mg/ml of the extracted solution) was mixed with a 200 μl of the working agent. The plate was sealed and allowed to incubate at 25 °C for 30 min. Absorbance was determined at 562 nm using a microplate reader (Biotek, Synergy HT). The results were compared with the BSA standard calibration plot and expressed in the unit of micrograms of proteins per a milliliter of a solution (μg/ml).

Lipolytic activity was examined based on the pNPB substrate. The protocol was slightly modified from the previous study [18]. Briefly, the pNPB solution (10 mM) was prepared in acetonitrile. This pNPB solution was mixed with ethanol and 50 mM potassium phosphate buffer (pH 7.5) at the final composition of 1:4:95 (pNPB:ethanol:phosphate buffer). Then, a 0.9 ml of this solution was mixed with 0.1 ml of the sample (1.4 mg/ml), prior to incubation at 37 °C for 60 min. The reaction was quenched by the addition of 2 ml absolute ethanol. The enzyme activity was measured at the UV-absorbance of 405 nm, in response to the production of *p*-nitrophenol (pNP). One unit of enzyme activity (U) was defined as the amount of enzyme that can release 1 μmol·min^{-1} of pNP under the assay conditions. This parameter was calculated by using the equation; $A = \varepsilon lc$, where the terms A, ε, l and C are the absorbance, the molar absorption coefficient (1.457×10^5 cm^2 mol^{-1}), the optical light path (1 cm), and the molar concentration, respectively [18].

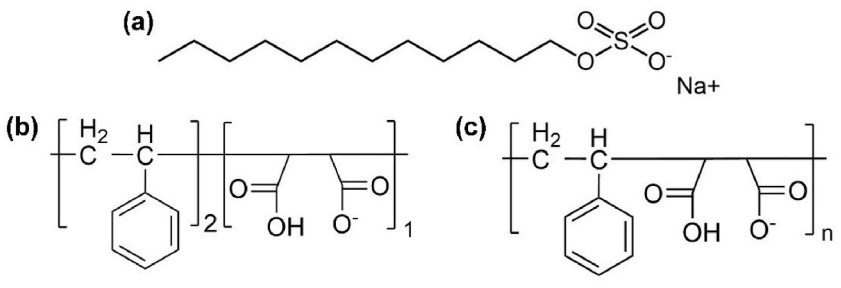

Fig. 1. Chemical structures of the membrane lysis agents at pH 7.5; (a) SDS, (b) 2000P and (c) photo-PSMA (or 1000P).

A combined technique of both scanning electron microscopy (SEM; TESCAN, MIRA4) and dynamic light scattering (DLS; SZ-100V2, HORIBA Instruments) was employed to evaluate the size diameter and morphological details of the end-state particles. For this, the freeze-dried sample was redissolved in Milli-Q water to obtain the concentration of 1.8% (w/v). The solution was sonicated in the ultrasonic bath (Crest Ultrasonics-690DAE) at 50 Hz for 15 min, followed by stirring for another 12 h. After filtration through a nylon filter membrane (0.45 μm), the sample was stirred for 12 h before measurement. For SEM testing, the sample was dropped onto the SEM stub, prior to air-drying for 48 h. Images were acquired after gold sputtering at an operating voltage and a working distance of 10 kV and 15 mm, respectively. The mean size was obtained by using ImageJ2 software analysis.

2.6. Statistical analysis

Statistical analysis was performed by using statistical software IBM SPSS statistics (Version 26) and expressed as the mean ± standard deviation. All data were based on a normal distribution. Their significant differences were analyzed by using one-way analysis of variance (ANOVA). When significant difference was found, differences among treatments were analyzed using multiple comparisons of means with Tukey's test.

3. Results and discussion

Copolymer of S and MAnh (PSMAnh) was successfully synthesized by photopolymerization using Irgacure® 2959 and carbon tetrabromide (CBr_4) as a radical initiator and a reversible chain transfer agent, respectively. Alkaline hydrolysis of this copolymer converted its anhydride ring into two carboxylic acid groups, rendering it into water-soluble format (PSMA) suited for cell lyse applications. The resultant copolymer product (referred to as photo-PSMA) shows the main ^{1}H-NMR peaks in Fig. 2a at 6.00–7.50 ppm, attributing to the aromatic five-protons (H5) of the styrene unit. In Fig. 2a, the characteristic peaks at 0.80–3.00 ppm, corresponding to the methine/methylene groups (H1, H2, H3 and H4) of the comonomers, are also detected. The presence of both aromatic proton signal and the methine/methylene backbone signals confirms the incorporation of S and MAnh along the copolymer backbone. These signals are also detected in 1000P (Figs. 2b) and 2000P (Fig. 2c). Thus, all three PSMA types (photo-PSMA, 1000P and 2000P) are the S/MAnh copolymer in nature.

DOSY-NMR technique was also used to confirm the successful PSMA synthesis. In Fig. 3, there is only one horizontal DOSY line appearing between the diffusion coefficient (LogD) values of −9.5 m^2/s and −10.0 m^2/s. Such DOSY signal is well-aligned with the ^{1}H-NMR resonances corresponding to the aromatic five-protons of styrene (δ6.00–7.50 ppm) and the aliphatic five-protons of the comonomer backbone (δ0.80–3.00 ppm). This reconfirms that the two comonomers are on the same molecule.

^{13}C-NMR spectroscopy was employed to evaluate the copolymer composition and the monomer sequence distribution in photo-PSMA, 1000P and 2000P. Due to a strong electron receiver characteristic, maleic anhydride (MAnh or 0) is less susceptible to undergo homopolymerization. Instead, it tends to copolymerise with styrene (S or 1) and gives an alternating S-MAnh copolymer. In Fig. 4 (inset), the quaternary aromatic carbon (C7) and the methylene carbon (C1) of styrene are known to be sensitive to the styrene-centered triad sequencing (010). When the mole fraction of MAnh nearly approaches the value of 0.9, the C1 and C7 resonances of the fully alternating triad sequencing (010) are expected at the chemical shifts of 32–37 ppm and 137–142 ppm, respectively [19]. This is

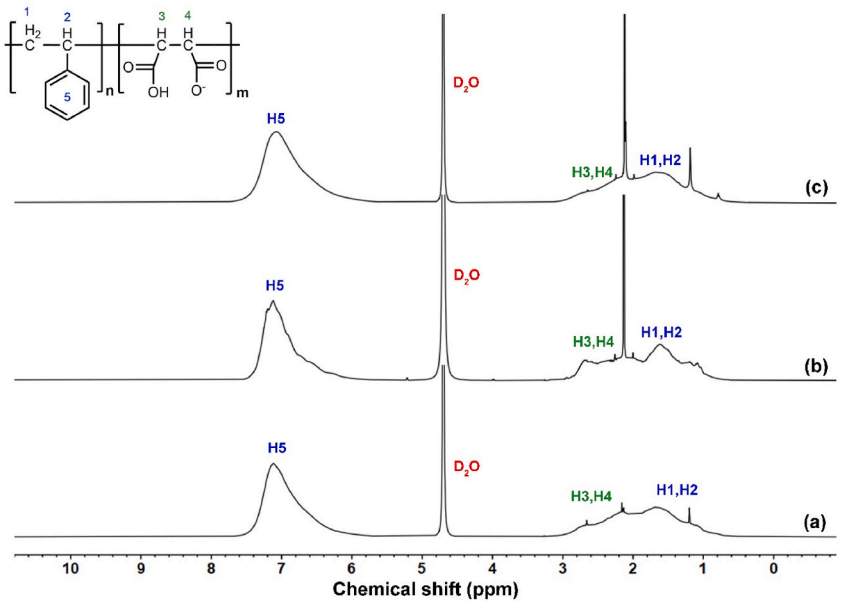

Fig. 2. ^{1}H-NMR Spectrum the hydrolysed PSMA samples in D_2O solvent; (a) photo-PSMA (b) 1000P and (c) 2000P.

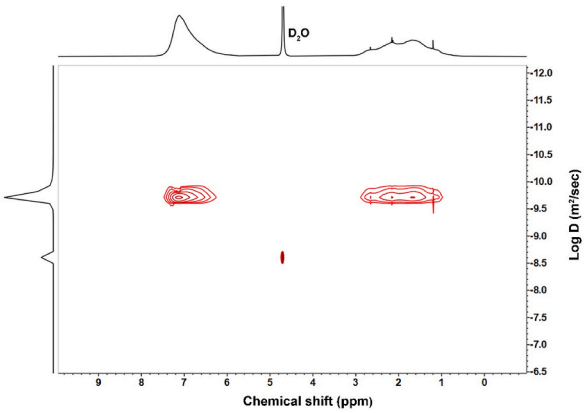

Fig. 3. DOSY ^{1}H-NMR Spectrum of our photo-PSMA in D_2O solvent.

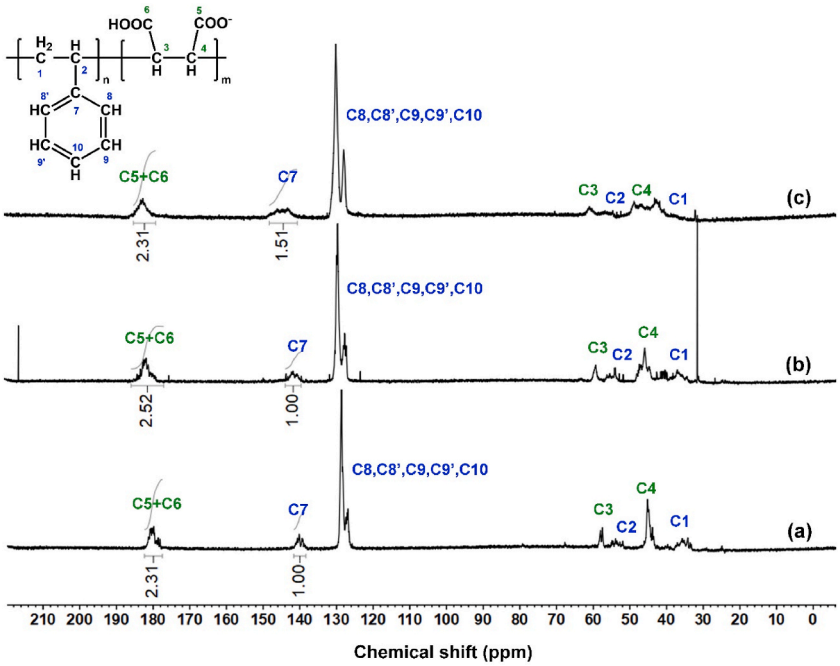

Fig. 4. ^{13}C-NMR Spectrum of different PSMAs in D_2O solvent; (a) photo-PSMA, (b) 1000P and (c) 2000P.

consistent with our results in Fig. 4a and b, confirming that photo-PSMA and 1000P are mainly alternating copolymer. With a fine structure like this, a multiplet C1 peak in Fig. 5a shows a strong spike (1 and 4) and a small one (2 and 3). These spikes are less intense in Fig. 5b (1000P). The spikes of the C1 peak was reported earlier in a very fine stereoregular PSMA derived from photo-copolymerization [19]. For 2000P in Figs. 4c and 5c, the C1 resonance at 32–37 ppm has become diminished. Comparing to photo-PSMA (Fig. 6a) and 1000P (Fig. 6b), the C7 resonance of 2000P in Fig. 6c is further shifted to the higher field region of 141–145 ppm, illustrating a preferential 110 or 011 sequence [20]. The 2000P sample is thus considered to be a semi-alternating rather than a complete alternating copolymer. As compared to 1000P and 2000P, the ^{13}C-NMR spectra of our photo-PSMA in Figs. 5 and 6 displays the more intense and well-resolved resonance lines. This demonstrates the better structural regularity along the copolymer backbone.

Taken into consideration that the monomer reactivity ratios for both comonomers are quite low (<0.02) and an equimolar S/MAnh polymerization was employed, it is generally accepted that the copolymer product is an almost alternating copolymer with the same 50:50 mol% composition as the comonomer feed [21]. To confirm this, the peak area integrations of the quaternary aromatic carbon (C7) at 137–142 ppm and the two MA carbonyl carbons (C5+C6) at 178–181 ppm in Fig. 4a for photo-PSMA were examined. The ratio of the peak integrations of I_{C7} and I_{C5+C6} in Fig. 4a is; I_{C7}:I_{C5+C6} = 1.00:2.31, which is close to the 1:2 ratio of the aromatic carbon in styrene (C7) and the two carbonyl carbons in MAnh (C5+C6). This suggests that the copolymer composition (S/MAnh) in photo-PSMA is around 50:50, implying that our in-house synthesized product has a strong tendency towards alternating copolymer. Furthermore, it

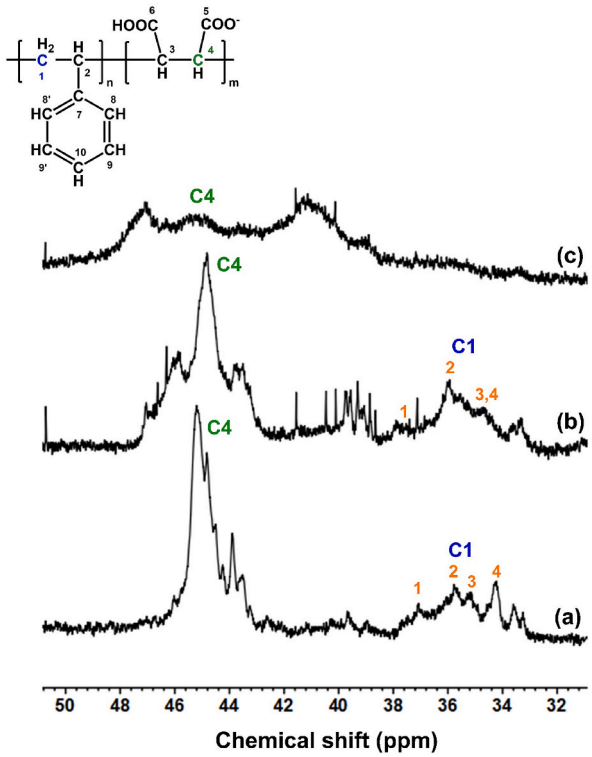

Fig. 5. Methylene/methine region of the ^{13}C-NMR spectrum for different PSMAs in D_2O solvent; (a) photo-PSMA, (b) 1000P and (c) 2000P.

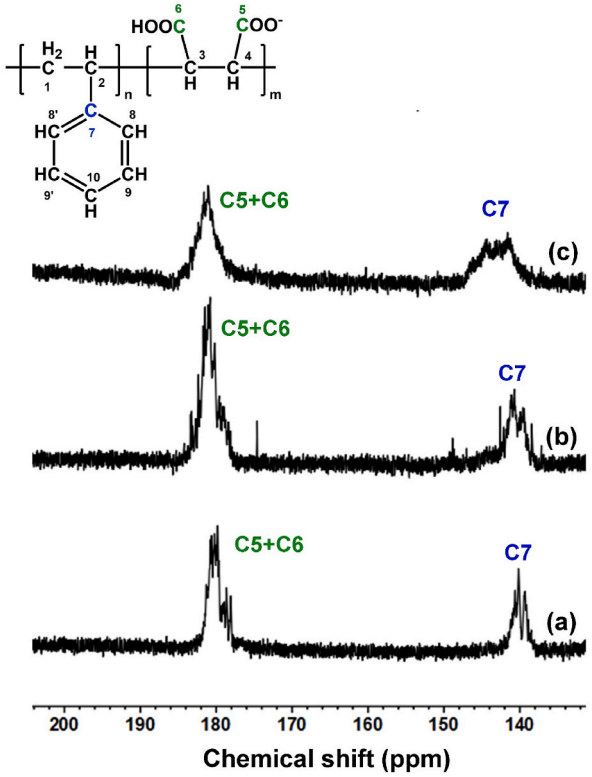

Fig. 6. Quaternary ^{13}C-NMR spectrum of the aromatic carbon C7 for different PSMAs in D_2O solvent; (a) photo-PSMA, (b) 1000P and (c) 2000P.

shows an acceptably low average-molecular weight (M_w) of 4.07 x 10^3 g/mol in Table .1. The value is closely comparable to that reported in our published work (4.90 x 10^3 g/mol) [17], suggesting that the photopolymerization technique employed herein is quite reliable and that the product obtained is acceptably reproducible. The ^{13}C-NMR analysis of 1000P in Figs. 4b and 2000P in Fig. 4c also reveals the copolymer composition of 44:56 mol% and 57:43 mol%, respectively. The unexpectedly low styrene content in 2000P can be associated with the loss of the styrene-rich segments during purification process via acetone precipitation described in section 2.2.

Implementation of photo-PSMA as a membrane lysis agent for soybean enzyme extraction was demonstrated for the first time in this study. The process was very simply and relied on seed soaking in aqueous-based media without any energy input or mechanical grinding. As such, soybean extraction was gently occurred without severe cell rupture or seed coat removal. The obvious change after soaking in the lysis solutions of photo-PSMA (Fig. 7a), 1000P (Figs. 7b), 2000P (Fig. 7c), SDS (Fig. 7d) and the control MOPS buffer (Fig. 7e) was the seed size increases due to water diffusion into cotyledon cells, oil bodies, protein storage vacuoles and intercellular spacing [22–24]. Water transport generally provides channels for cytoplasmic solutes to pass across cellular membrane. In the presence of membrane pore defects, diffusion of the solutes to the surrounding is highly occurred. This may be the cause for the increased recovery yields in all PSMA systems in Fig. 8, comparing to the SDS extraction and the control ($p < 0.01$). Formation of larger micropore defects during PSMA extractions may be related to the enhanced hydrophobic interactions between the lipid acyl chains and the aromatic rings of the copolymers. Evidence of the PSMA-induced pore formation on the soybean lipid film was recently demonstrated. The large uncovered surface areas of 0.5–3.9 μm in size were detected after exposure to 0.5% PSMA solution [25].

Determination of the total sugar content was performed by the phenol-sulfuric method using glucose as a standard. The results are present in Fig. 9. Comparing to the control ($p < 0.001$), extractions by the three PSMAs and SDS yield higher total sugar contents. The maximum value is obtained by the SDS extraction, implying its non-selectivity for protein recovery purposes. Beside phenol-sulfuric test, the bicinchoninic acid (BCA) assay was also employed to quantify the total protein content in the extracted samples. This method involves reduction of cupric ions (Cu^{2+}) to cuprous ion (Cu^{+}) by the peptide bonds, followed by chelation of Cu^{+} with BCA molecules. The final complexes give an intense purple blue color with a UV peak absorbance at 562 nm. The assay generally gives guideline to a broad spectrum of water-soluble proteins, rather than a specific protein group. In Fig. 10, the extracted solutions of SDS and the control exhibit the total protein content around 26–27 μg/ml, significantly higher than those of photo-PSMA, 1000P and 2000P ($p < 0.001$). However, this does not necessarily mean the greater extractability towards lipolytic enzymes of interest. To confirm this, evaluation of the lipolytic activity based on the pNPB substrate was carried out. By dividing the resultant lipolytic activity with the BCA protein content in Fig. 9, the more precise term, namely a specific lipolytic activity, was obtained. The results are presented in Fig. 11. The higher specific lipolytic activity, the purer fraction of the targeted enzymes does the sample possess. Despite the highest contents of both sugars in Fig. 9 and proteins in Fig. 10, extraction by SDS in Fig. 11 yields the lowest specific enzyme activity. The value is as low as the control ($P = 0.054$). Taken into consideration that the SDS critical micelle concentration is lesser than the SDS concentration used in this study (1% w/v) [26,27], there may be possibility of surfactant-protein binding occurred under the experimental employed. A permanent binding with the SDS molecules can alter the protein native structures, resulting in the loss of enzymatic function as observed for SDS in Fig. 11. In the presence of photo-PSMA, 1000P or 2000P, this incident seems to be suppressed. The three PSMA-based solutions in Fig. 11 exhibit the increased specific lipolytic activity, at least 2.7 times greater than the other two systems. As such, there may be certain stabilization effect that helps to protect the detached enzymes from structural changes and becoming denaturation.

The key function of surfactants to lyse biological membrane and release plant bioactive compounds depends on their amphipathic character that allows them to properly interact with the cell membranes. As proposed by Lichtenberg and coworkers [28], the molecules of surfactant initially adsorb and saturate on the outer membrane leaflet. If they are available in excess and possess moderate hydrophobicity, they can then further flip into the membrane layer and induce micropore defect formation. This step is usually accompanied by a slow leakage of cytoplasmic components, such as lipolytic enzymes. Once detached from biological cells, they need to be transferred to a protective reservoir to avoid undesirable chemical reactions and denaturation. PSMA self-aggregates may somehow create such environment. As noticed in the DLS plots in Fig. 12, the extracted solutions of photo-PSMA and 1000P are composed of particles with the Z-average diameters around 159.0 ± 7.3 nm (black) and 132.5 ± 3.6 nm (red), respectively. For those of 2000P particles (blue), they possess the increased Z-average diameter around 226.2 ± 15.8 nm. The results are in good agreement with the previous studies, wherein a number of therapeutic agents were immobilized inside the PSMA micelles, including curcumin derivatives [29], bio-based wax [30], paclitaxel [31] and temoporfin [32]. PSMA micellization is generally driven by the unfavorable interactions between the water molecules and its aromatic ring. The hydrophobic styrene units are expected to be buried within the micellar core region, while those of the polar MA units be located at the water-particle boundary to maximize the hydrogen bonding with the water molecules. The core region of these particles is considered to be hydrophobic in nature, allowing certain compounds to be immobilized and shielded from the external stimuli factors. Comparing to typical lipid nanodiscs whose size diameters were

Table 1
Various physical properties of different PSMA sources.

Sample	Molar S:MA ratio[a]	M_w[b] (g/mol)	M_n[b] (g/mol)	PDI[b]
Photo-PSMA	46:54	4.07 x 10^3	2.68 x 10^3	1.52
1000P	44:56	2.10 x 10^3	1.53 x 10^3	1.37
2000P	57:43	4.53 x 10^3	2.84 x 10^3	1.59

[a] Data obtained by ^{13}C-NMR analysis.
[b] GPC data based on the non-hydrolysed samples.

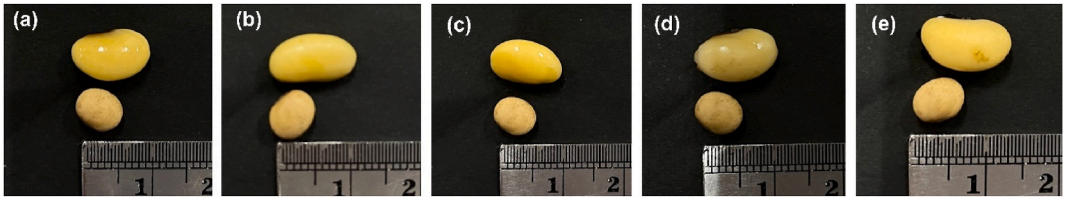

Fig. 7. Morphological changes of soybean seeds after overnight soaking in the pH 7.5 phosphate buffer solutions containing different lysis agents; (a) photo-PSMA, (b) 1000P, (c) 2000P and (d) SDS. Result of the surfactant-free solution (control) was also compared in (e).

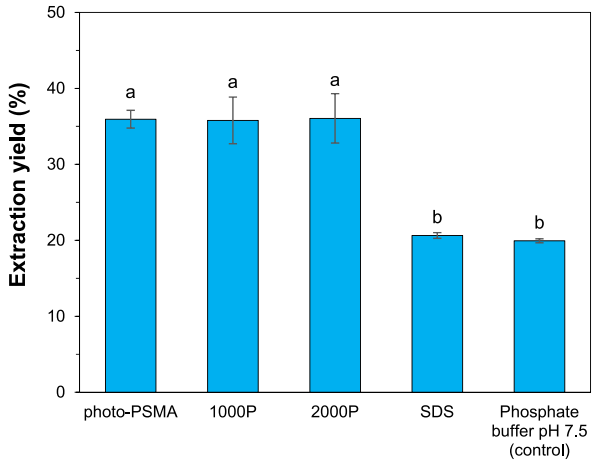

Fig. 8. Percentages (mean ± SD) of the extraction yields for different extracted solutions. Bars with different letters are significantly different at $P < 0.05$.

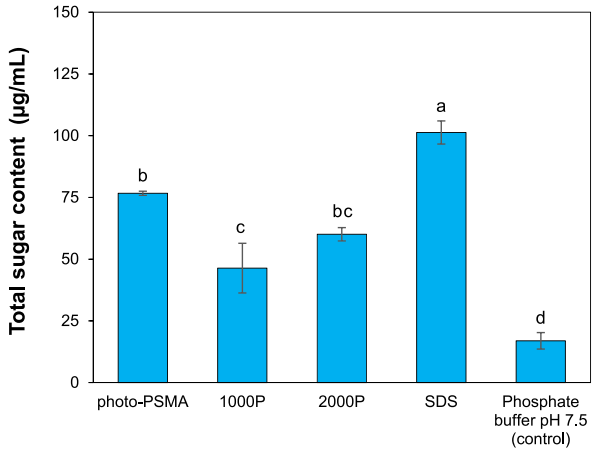

Fig. 9. Total sugar contents (mean ± SD) of the extracted solutions obtained from different extracting systems. Bars with different letters are significantly different at $P < 0.05$.

reported between 10 and 25 nm [8,9,12,25,33], our end-state particles in Fig. 12 are much larger in size. As such, these particles may not represent an ideal membrane-like structure for advanced biophysical and structural biology characterization. Formation of the very fine lipid nanodiscs requires the balanced lipid/PSMA proportion [34,35], which may not be realistic under the experimental conditions employed. Without exogenous phospholipid or incomplete membrane solubilization, availability of the lipid patches to complex with the PSMA chains and form a thermodynamically stable lipid nanodisc is rather limited. Another important factor affecting formation of such nanodisc is a lipid type of which it was contained. Solubilization of the Gram-negative *E. coli* membranes upon PSMA addition yielded the nanodiscs with the size diameter of around 10 nm, while that of the Gram-positive *B. subtilis* membranes showed larger size between 50 and 100 nm [36]. Taken together with the DLS results in Fig. 12, possibility in obtaining the

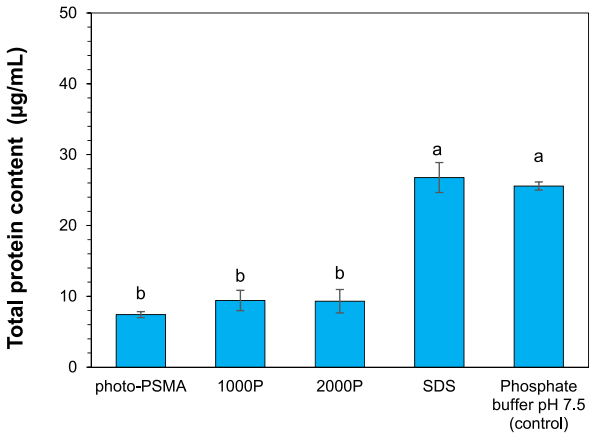

Fig. 10. Total protein contents (mean ± SD) of the extracted solutions obtained from different extracting systems. Bars with different letters are significantly different at $P < 0.05$.

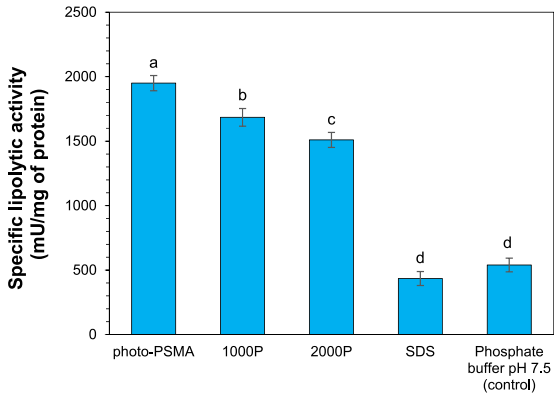

Fig. 11. Specific lipolytic activity (mean ± SD) of the extracted solutions obtained from different extracting systems. Bars with different letters are significantly different at $P < 0.05$.

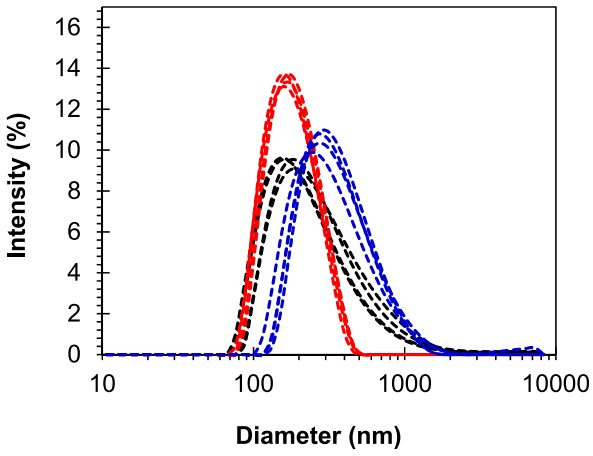

Fig. 12. DLS plots of the extracted solutions using photo-PSMA (black), 1000P (red) or 2000P (blue) as a membrane lysis agent. (For interpretation of the references to color in this figure legend, the reader is referred to the Web version of this article.)

lipid/PSMA/protein complexes in this study should not be completely ignored. Nonetheless, additional experiments need to be performed to clarify this matter.

Besides DLS technique, the scanning electron microscopy (SEM) was also used to access morphological detail of the particles in Fig. 12, as well as to approximate their size diameters. For each selected unit in Fig. 13 (labelled as 1, 2, 3, 4, 5, 6, 7, 8, 9 or 10), the particle size was examined by using the ImageJ analysis software. The values were averaged and presented as the mean size diameter. As noticed in Fig. 13a (photo-PSMA), Fig. 13b (1000P) and Fig. 13c (2000P), the smallest units in the extracted solutions appear spherical round shape (circles). These particles show the mean size diameters of 39.5 ± 6.7 nm (for photo-PSMA), 77.4 ± 18.6 nm (for 1000P) and 118.2 ± 25.7 nm (for 2000P). They intend to self-aggregate into larger size dimensions (rectangles in Fig. 13), suggesting a limited shelf-life stability under dehydrated storage conditions. Similar PSMA aggregates were previously reported by a number of researchers [37–39]. With the increased styrene content in 2000P, particle aggregation even leads to vesicular network formation in Fig. 13c (dashed with arrows). For the SDS system in Fig. 13d, their end-state particles display a flower-like morphology constructed by layers of micron-sized rods. This microrod flower is also found in the control (data not showed), suggesting possibility of supramolecular assemblies of soybean biomolecules, rather than the SDS complexation. Moreover, there was no sign of round shape nanovesicle in the SEM images for the control and SDS (Fig. 13d). Without a shielding effect of the vesicular PSMA reservoirs, soybean enzymes may have been directly exposure to the external stimuli (e.g., oxygen gas, buffer salts, heat, etc.) and experience higher risks of chemical and structural changes. This would lead to protein denaturation and loss of catalytic activity, as convinced by the reduced specific lipolytic activity in the SDS and control samples in Fig. 11.

Interestingly, we observed the increased specific enzyme activity in the samples of photo-PSMA and 1000P in comparison to the 2000P sample. This is quite different from most of the previous published studies [40–42]. It is unclear what causes the worsening of 2000P. Regardless, we believed that this can be explained by the reduced ability of the hydrophilic peptide segments, comprising of aspartic acid, glutamic acid and/or lysine amino acids [43], to insert within the more hydrophobic core of the 2000P vesicles comparing to those of the two 1:1 PSMA types. Another possible reason can be drawn by the NMR analysis in Figs. 4, Figs. 5 and 6. The more random architecture of 2000P may hinder its binding effect with the immobilized enzymes, as convinced by the increased Z-average diameter in Fig. 12. In this situation, the immobilized enzymes are still capable of interacting with the external stimuli factors and can still undergo some chemical reactions, causing them to change their native structure and lose their lipolytic activity. This may be the reason for the reduced specific lipolytic activity of 2000P comparing to photo-PSMA and 1000P in Fig. 11. Another question arisen as why the using of photo-PSMA shows better extraction performance than 1000P in Fig. 11. Taken into consideration that these two have almost the same values of S:MA mol% in Table .1 and they both produce similar particle sizes in Fig. 12, difference in their performance may be a consequence of photo-initiated method. Upon irradiation, Irgacure® 2959 in Fig. 14a undergoes photodissociation producing two free radicals. Since benzoyl radical is more reactive than the ketyl radical, it intends to initiate chain propagation and yields the hydroxyl-terminated chains (Fig. 14b). As suggested by the previous research study [15], this chain-end can facilitate different binding effect comparing to those commercial PSMA sources. Assuming that 1000P was made by benzoyl peroxide (BPO) initiator and that it carries the BPO-end, folding this BPO-terminated segment into the hydrophobic core of the PSMA aggregates would be easier than that of the hydroxyl-terminated end of photo-PSMA. Whilst this BPO-terminal chain helps to stabilize the 1000P

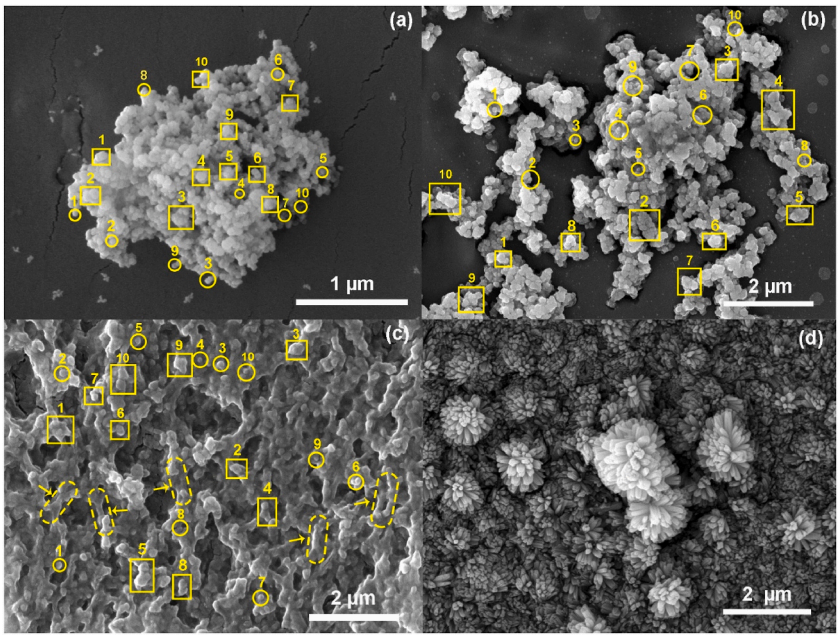

Fig. 13. SEM images of the end-state particles obtained by using different membrane agents; (a) photo-PSMA, (b) 1000P, (c) 2000P and (d), SDS. Image in (a) and (b)–(d) were taken at the magnifications of 50.0 kx and 20.0 kx, respectively.

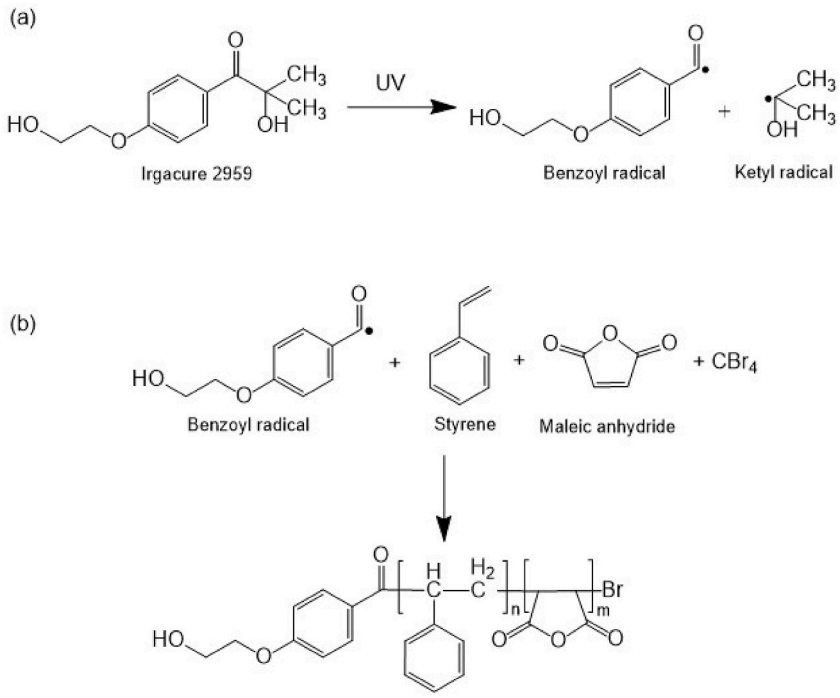

Fig. 14. Proposed mechanisms for; (a) photodissociation of Irgacure® 2959 and (b) synthesis of photo-PSMAnh with hydroxyl-terminated end.

vesicles, structural integrity of the immobilized enzymes inside the vesicles can be disturbed by their proximate interactions. This can modify the local environment around the catalytic lid domains of the enzymes, causing them to lose their biological function as in the case of 1000P comparing to photo-PSMA in Fig. 11. This postulation should be treated cautiously as it excludes a number of variables involved, such as types and chemical natures of the immobilized enzymes, polymer molecular weights and the styrene block length, ionic strength, degree of ionization and potent interactions with the buffer agents.

Overall results illustrated that soybean lipolytic enzymes could be recovered directly into nanovesicles by seed soaking in the PSMA lysis solution. The process was simply occurred in aqueous media with no use of energy input or toxic organic solvent, thus representing alternative greener extraction protocol for a large-scale production of industrial plant enzymes. Without exogeneous phospholipids or incomplete membrane solubilization (via severe mechanical grinding), formation of an ideal lipid nanodisc with a very fine nanometric-sized diameter (5–25 nm) was hardly achieved. Nonetheless, PSMA self-aggregates could serve as an alternative reservoir for enzyme immobilization, thus protecting the biocatalysts from undesirable side reactions. However, the usefulness of this protocol depends on the ability of the PSMA aggregates to solubilize the targeted proteins. With the very fine structural regularity and the precisely-balanced hydrophobic/hydrophilic groups in the photo-PSMA structure, immobilization of soybean proteins into the styrene core of the aggregates could be occurred with a minimum repulsion effect. The decreased Z-average diameters for the 1:1 PSMA vesicles (photo-PSMA and 1000P) as compared to that of 2000P (Fig. 12) together with the enhanced specific enzyme activity by the 1:1 PSMA extractions (Fig. 11), added support for the need of amphipathic PSMA type (50:50 mol%) in recovery of soybean lipolytic enzymes. This was different from the previous studies in which the 2:1 PSMA was more preferable [40–42]. As such, our method may be suitable for certain protein types, such as those amphipathic soybean esterases and lipases, but not for a wider range of membrane protein systems. Systematic investigation on different enzymes needs to be performed in the future to generalize the possible applications of the photo-PSMA lysis agent, especially through the use of controlled polymerization technique.

4. Conclusion

PSMA membrane lysis agent with improved structural regularity was synthesized by photopolymerization using CBr_4 as a reversible chain transfer agent. This copolymer (photo-PSMA) was applied for the first time in a recovery of soybean lipolytic enzymes. Extraction by all PSMA sources (photo-PSMA, 1000P and 2000P) could render the enzymes directly into the nanometric-sized particles (130–240 nm). The process was believed to be driven by the PSMA self-aggregation in an aqueous media. The hydrophobic core of these nanostructures could serve as a protection reservoir for the detached enzymes to be resided, protected and resolved in their full functioning state. With the precisely-balanced hydrophobic/hydrophilic groups along the polymer backbone (50:50 mol% of S/MA) and at the chain-end, immobilization of soybean enzymes within the photo-PSMA vesicles was greatly achieved with a minimal repulsion effect. This was convinced by the small particle size range (130–166 nm) and the greatest specific lipolytic activity (1,950 mU/mg), comparing to the most commonly used 2000P lysis agent. Our in house-synthesized PSMA lysis agent had thus demonstrated its great potential in cell lyse applications, especially for the extraction of amphipathic lipolytic enzymes from soybean seeds.

Funding

This work was supported by Mae Fah Luang University [grant no. 631B01013 and no. 652A01013]. One of our co-authors (Miss Chatmani Buachi) also received a tuition scholarship from Mae Fah Luang University [grant no. 037]. This project has received funding from the European Union's Horizon 2020 research and innovation programme under the Marie Skłodowska-Curie grant agreement No 871650.

Data availability statement

The data that support the findings of this study are available on request from the corresponding author.

CRediT authorship contribution statement

Chatmani Buachi: Methodology, Investigation, Formal analysis. **Kamonchanok Thananukul:** Methodology, Investigation, Formal analysis. **Kitiphong Khongphinitbunjong:** Writing – original draft, Formal analysis. **Robert Molloy:** Writing – review & editing, Supervision, Methodology, Conceptualization. **Patchara Punyamoonwongsa:** Writing – review & editing, Writing – original draft, Validation, Methodology, Funding acquisition, Formal analysis, Conceptualization.

Declaration of competing interest

The authors declare that they have no known competing financial interests or personal relationships that could have appeared to influence the work reported in this paper.

Acknowledgements

The authors wish to thank Prof. Brian Tighe and Prof. Paul Topham (Aston University, UK) for their insightful comments and suggestions. The authors also wish to thank Miss Daranee Pudta and the Scientific and Technological Instruments Center, Mae Fah Luang University for the NMR analysis and laboratory facilities.

References

[1] M. Barros, G. Macedo, Biochemical characterization of esterase from soybean (Glycine max L.), Food Sci. Biotechnol. 20 (5) (2011).
[2] A. Houde, A. Kademi, D. Leblanc, Lipases and their industrial applications: an overview, Appl. Biochem. Biotechnol. 118 (2004) 155–170.
[3] D.L. Ollis, E. Cheah, M. Cygler, B. Dijkstra, F. Frolow, S.M. Franken, M. Harel, S.J. Remington, I. Silman, J. Schrag, The α/β hydrolase fold, Protein Eng. Des. Sel. 5 (3) (1992) 197–211.
[4] K. Vivek, G. Sandhia, S. Subramaniyan, Extremophilic lipases for industrial applications: a general review, Biotechnol. Adv. 60 (2022) 108002.
[5] M. Barros, L. Fleuri, G. Macedo, Seed lipases: sources, applications and properties-a review, Braz. J. Chem. Eng. 27 (2010) 15–29.
[6] C.W. Bair, Microscopy of Soybean Seeds: Cellular and Subcellular Structure during Germination, Development and Processing with Emphasis on Lipid Bodies, Iowa State University, 1979.
[7] V. Pata, F. Ahmed, D.E. Discher, N. Dan, Membrane solubilization by detergent: resistance conferred by thickness, Langmuir 20 (10) (2004) 3888–3893.
[8] Y. Guo, Detergent-free systems for structural studies of membrane proteins, Biochem. Soc. Trans. 49 (3) (2021) 1361–1374.
[9] S. Paulin, Surfactant-free purification of membrane protein complexes from bacteria: application to the staphylococcal penicillin-binding protein complex PBP2/PBP2a, Nanotechnology 25 (2014) 1–7.
[10] P. Punyamoonwongsa, Lipid nanodiscs of poly (styrene-alt-maleic acid) to enhance plant antioxidant extraction, E-Polymers 22 (1) (2022) 607–614.
[11] C. Buachi, C. Thammachai, B.J. Tighe, P.D. Topham, R. Molloy, P. Punyamoonwongsa, Encapsulation of propolis extracts in aqueous formulations by using nanovesicles of lipid and poly (styrene-alt-maleic acid), Artif. Cell Nanomed. Biotechnol. 51 (1) (2023) 192–204.
[12] K.A. Morrison, L. Wood, K.J. Edler, J. Doutch, G.J. Price, F. Koumanov, P. Whitley, Membrane extraction with styrene-maleic acid copolymer results in insulin receptor autophosphorylation in the absence of ligand, Sci. Rep. 12 (1) (2022) 3532.
[13] S.D. Sütekin, A.B. Atıcı, O. Güven, A.S. Hoffman, Controlling of free radical copolymerization of styrene and maleic anhydride via RAFT process for the preparation of acetaminophen drug conjugates, Radiat. Phys. Chem. 148 (2018) 5–12.
[14] D.C. Wu, C.Y. Hong, C.Y. Pan, W.D. He, Study on controlled radical alternating copolymerization of styrene with maleic anhydride under UV irradiation, Polym. Int. 52 (1) (2003) 98–103.
[15] G.M. Neville, K.A. Morrison, E.R. Shilliday, J. Doutch, R. Dalgliesh, G.J. Price, K.J. Edler, The effect of polymer end-group on the formation of styrene–maleic acid lipid particles (SMALPs), Soft Matter 19 (44) (2023) 8507–8518.
[16] G. Odian, Principles of Polymerization, John Wiley & Sons, 2004.
[17] T. Khaojanta, W. Kalaithong, R. Somsunan, P. Punyamoonwongsa, A. Mahomed, P.D. Topham, B.J. Tighe, R. Molloy, Synthesis and characterization of block copolymers of styrene-maleic acid with acrylamide and N, N-dimethylacrylamide, Polym. Eng. Sci. 62 (6) (2022) 2031–2046.
[18] D.-W. Lee, Y.-S. Koh, K.-J. Kim, B.-C. Kim, H.-J. Choi, D.-S. Kim, M.T. Suhartono, Y.-R. Pyun, Isolation and characterization of a thermophilic lipase from Bacillus thermoleovorans ID-1, FEMS (Fed. Eur. Microbiol. Soc.) Microbiol. Lett. 179 (2) (1999) 393–400.
[19] P.F. Barron, D.J. Hill, J.H. O'Donnell, P.W. O'Sullivan, Applications of DEPT experiments to the carbon-13 NMR of copolymers: poly (styrene-co-maleic anhydride) and poly (styrene-co-acrylonitrile), Macromolecules 17 (10) (1984) 1967–1972.
[20] N.T.H. Ha, Determination of triad sequence distribution of copolymers of maleic anhydride and its derivates with donor monomers by 13C nmr spectroscopy, Polymer 40 (4) (1999) 1081–1086.
[21] A. Rudin, P. Choi, The Elements of Polymer Science and Engineering, Academic press, 2012.
[22] K. Lechowska, S. Kubala, Ł. Wojtyla, G. Nowaczyk, M. Quinet, S. Lutts, M. Garnczarska, New insight on water status in germinating Brassica napus seeds in relation to priming-improved germination, Int. J. Mol. Sci. 20 (3) (2019) 540.
[23] D.J. Parrish, A.C. Leopold, Transient changes during soybean imbibition, Plant Physiol. 59 (6) (1977) 1111–1115.
[24] S.H. Duke, G. Kakefuda, T.M. Harvey, Differential leakage of intracellular substances from imbibing soybean seeds, Plant Physiol. 72 (4) (1983) 919–924.
[25] M.O. Rydmark, M.K. Christensen, E.S. Köksal, I. Kantarci, K. Kustanovich, V. Yantchev, A. Jesorka, I. Gözen, Styrene maleic acid copolymer induces pores in biomembranes, Soft Matter 15 (39) (2019) 7934–7944.

[26] J. Juan-Colás, L. Dresser, K. Morris, H. Lagadou, R.H. Ward, A. Burns, S. Tear, S. Johnson, M.C. Leake, S.D. Quinn, The mechanism of vesicle solubilization by the detergent sodium dodecyl sulfate, Langmuir 36 (39) (2020) 11499–11507.
[27] A.K. Bhuyan, On the mechanism of SDS-induced protein denaturation, Biopolymers: Original Research on Biomolecules 93 (2) (2010) 186–199.
[28] D. Lichtenberg, H. Ahyayauch, F.M. Goñi, The mechanism of detergent solubilization of lipid bilayers, Biophys. J. 105 (2) (2013) 289–299.
[29] O. Martey, M. Nimick, S. Taurin, V. Sundararajan, K. Greish, R.J. Rosengren, Styrene maleic acid-encapsulated RL71 micelles suppress tumor growth in a murine xenograft model of triple negative breast cancer, Int. J. Nanomed. (2017) 7225–7237.
[30] P. Samyn, V.K. Rastogi, Stabilization of an aqueous bio-based wax nano-emulsion through encapsulation, Nanomaterials 12 (23) (2022) 4329.
[31] N.N. Parayath, H. Nehoff, S.E. Norton, A.J. Highton, S. Taurin, R.A. Kemp, K. Greish, Styrene maleic acid-encapsulated paclitaxel micelles: antitumor activity and toxicity studies following oral administration in a murine orthotopic colon cancer model, Int. J. Nanomed. (2016) 3979–3991.
[32] J. Fang, S. Gao, R. Islam, H. Nema, R. Yanagibashi, N. Yoneda, N. Watanabe, Y. Yasuda, N. Nuita, J.-R. Zhou, Styrene maleic acid copolymer-based micellar formation of temoporfin (SMA@ mTHPC) behaves as a nanoprobe for tumor-targeted photodynamic therapy with a superior safety, Biomedicines 9 (10) (2021) 1493.
[33] A. Helenius, K. Simons, Solubilization of membranes by detergents, Biochim. Biophys. Acta Rev. Biomembr. 415 (1) (1975) 29–79.
[34] S. Scheidelaar, M.C. Koorengevel, J.D. Pardo, J.D. Meeldijk, E. Breukink, J.A. Killian, Molecular model for the solubilization of membranes into nanodisks by styrene maleic acid copolymers, Biophys. J. 108 (2015) 279–290.
[35] P.S. Orekhov, M.E. Bozdaganyan, N. Voskoboynikova, A.Y. Mulkidjanian, M.G. Karlova, A. Yudenko, A. Remeeva, Y.L. Ryzhykau, I. Gushchin, V.I. Gordeliy, Mechanisms of formation, structure, and dynamics of lipoprotein discs stabilized by amphiphilic copolymers: a comprehensive review, Nanomaterials 12 (3) (2022) 361.
[36] P.A. de Jonge, D.J. Smit Sibinga, O.A. Boright, A.R. Costa, F.L. Nobrega, S.J. Brouns, B.E. Dutilh, Development of styrene maleic acid lipid particles as a tool for studies of phage-host interactions, J. Virol. 94 (23) (2020), https://doi.org/10.1128/jvi.01559-20.
[37] A.F. Craig, E.E. Clark, I.D. Sahu, R. Zhang, N.D. Frantz, M.S. Al-Abdul-Wahid, C. Dabney-Smith, D. Konkolewicz, G.A. Lorigan, Tuning the size of styrene-maleic acid copolymer-lipid nanoparticles (SMALPs) using RAFT polymerization for biophysical studies, Biochim. Biophys. Acta Biomembr. 1858 (11) (2016) 2931–2939.
[38] K.M. Burridge, B.D. Harding, I.D. Sahu, M.M. Kearns, R.B. Stowe, M.T. Dolan, R.E. Edelmann, C. Dabney-Smith, R.C. Page, D. Konkolewicz, Simple derivatization of RAFT-synthesized styrene–maleic anhydride copolymers for lipid disk formulations, Biomacromolecules 21 (3) (2020) 1274–1284.
[39] J.J.D. Pardo, M.C. Koorengevel, N. Uwugiaren, J. Weijers, A.H. Kopf, H. Jahn, C.A. van Walree, M.J. van Steenbergen, J.A. Killian, Membrane solubilization by styrene-maleic acid copolymers: delineating the role of polymer length, Biophys. J. 115 (1) (2018) 129–138.
[40] K.A. Morrison, A. Akram, A. Mathews, Z.A. Khan, J.H. Patel, C. Zhou, D.J. Hardy, C. Moore-Kelly, R. Patel, V. Odiba, Membrane protein extraction and purification using styrene–maleic acid (SMA) copolymer: effect of variations in polymer structure, Biochem. J. 473 (23) (2016) 4349–4360.
[41] M.C. Fiori, W. Zheng, E. Kamilar, G. Simiyu, G.A. Altenberg, H. Liang, Extraction and reconstitution of membrane proteins into lipid nanodiscs encased by zwitterionic styrene-maleic amide copolymers, Sci. Rep. 10 (1) (2020) 9940.
[42] O. Korotych, J. Mondal, K.M. Gattás-Asfura, J. Hendricks, B.D. Bruce, Evaluation of commercially available styrene-co-maleic acid polymers for the extraction of membrane proteins from spinach chloroplast thylakoids, Eur. Polym. J. 114 (2019) 485–500.
[43] Z.-i. Yokoyama, H. Hirai, Purification and molecular properties of soybean esterase, Agric. Biol. Chem. 51 (1) (1987) 259–260.